*atmosphere*

MDPI

*Article*

# Cloudiness Information Services for Solar Energy Management in West Africa

**Derrick Kwadwo Danso [1,2,*], Sandrine Anquetin [1], Arona Diedhiou [1,2] and Rabani Adamou [3]**

1 Université Grenoble Alpes, IRD, CNRS, Grenoble-INP, IGE, 38000 Grenoble, France; sandrine.anquetin@univ-grenoble-alpes.fr (S.A.); arona.diedhiou@ird.fr (A.D.)
2 Laboratoire de Physique de l'Atmosphère et de Mécaniques des Fluides (LAPAMF), Université Félix Houphoüet Boigny, Abidjan 22 BP 582, Cote d'Ivoire
3 WASCAL GRP on Climate Change and Energy, Faculté des Sciences et Techniques, Université Abdou Moumouni, Niamey 10662, Niger; adamrabani@yahoo.fr
* Correspondence: derrick.danso@univ-grenoble-alpes.fr

Received: 5 August 2020; Accepted: 12 August 2020; Published: 13 August 2020


**Abstract:** In West Africa (WA), interest in solar energy development has risen in recent years with many planned and ongoing projects currently in the region. However, a major drawback to this development in the region is the intense cloud cover that reduces the incoming solar radiation when present and causes fluctuations in solar power production. Therefore, understanding the occurrence of clouds and their link to the surface solar radiation in the region is important for making plans to manage future solar energy production. In this study, we use the state-of-the-art European Centre for Medium-range Weather Forecasts ReAnalysis (ERA5) dataset to examine the occurrence and persistence of cloudy and clear-sky conditions in the region. Then, we investigate the effects of cloud cover on the quantity and variability of the incoming solar radiation. The cloud shortwave radiation attenuation ($CRA^{\downarrow}_{SW}$) is used to quantify the amount of incoming solar radiation that is lost due to clouds. The results showed that the attenuation of incoming solar radiation is stronger in all months over the southern part of WA near the Guinea Coast. Across the whole region, the maximum attenuation occurs in August, with a mean $CRA^{\downarrow}_{SW}$ of about 55% over southern WA and between 20% and 35% in the Sahelian region. Southern WA is characterized by a higher occurrence of persistent cloudy conditions, while the Sahel region and northern WA are associated with frequent clear-sky conditions. Nonetheless, continuous periods with extremely low surface solar radiation were found to be few over the whole region. The analysis also showed that the surface solar radiation received from November to April only varies marginally from one year to the other. However, there is a higher uncertainty during the core of the monsoon season (June to October) with regard to the quantity of incoming solar radiation. The results obtained show the need for robust management plans to ensure the long-term success of solar energy projects in the region.

**Keywords:** cloud cover; solar energy; surface solar radiation; attenuation; West Africa; ERA5

## 1. Introduction

According to the fifth assessment report of the Intergovernmental Panel on Climate Change (IPCC), concentrations of greenhouse gases (GHGs) have risen in recent times with a 40% increase in $CO_2$ concentration since pre-industrial times [1]. This has led to the observed warming of the earth's surface and atmosphere. In 2017, anthropogenic warming due to GHG emissions reached about 1 °C above pre-industrial levels [2]. Nearly two-thirds of all GHG emissions emanate from the energy sector [3], which is primarily due to the combustion of fossil fuels such as coal and petroleum. With growing

demands for energy due to economic growth around the world, continued GHG emissions will lead to further warming of the earth's atmosphere. However, the Paris Agreement was made in 2015 to ensure that the rise in global average temperature is kept below 2 °C above the pre-industrial levels within this century. As a result, one of the major global responses has been to develop and/or increase the consumption of renewable energies such as solar energy, while reducing fossil energy use [4].

In West Africa (WA), projects dealing with solar energy development and implementation have attracted lots of interest from many governments and industries since the Paris Agreement due to the high potential for solar power generation in the region [5,6]. Countries such as Ghana and Cote d'Ivoire are currently undergoing significant economic and infrastructural developments; thus, the need for clean energy keeps increasing. For instance, in Cote d'Ivoire, the national renewable energy policy is focused on increasing the contribution of variable renewables to total electricity generation up to 16% by 2030. Consequently, a 25 MW solar photovoltaic (PV) power plant is currently under construction in northern Cote d'Ivoire, while two other 30 MW capacity plants have been approved for construction in the northwestern part of the country [7]. In Ghana, a 155 MW capacity solar PV power plant is currently under construction in the southwestern part of the country and will be the largest solar farm in the WA region when completed [8]. In addition, there are many planned and existing solar energy projects in the Sahelian region of WA. These include the 33 MW capacity Zagtouli solar PV power plant in Burkina Faso [9], which is currently the largest operational PV plant in the Sahelian region of WA.

Despite the high solar resource availability in the region [5,6], the large-scale development of solar energy such as in a 100% off-grid solar PV system could seriously be hindered by drawbacks associated with crustal dust and cloud cover. When present, dust and cloud cover strongly decrease the surface solar radiation available for solar power generation [10–12]. In West Africa, some studies (e.g., [12,13]) have investigated the impacts of dust on the efficiency of PV modules and solar power production, but very little has been done on clouds in a similar context. Clouds largely drive the albedo of the atmosphere that determines the amount of solar radiation reaching the earth's surface during the daytime [14]. Additionally, the temporal evolution of clouds controls the variability of the incoming solar radiation [15,16]. Thus, understanding the impacts of clouds on the availability and evolution of surface solar radiation in WA is essential for the successful integration of solar energy in the regional power pool. This could help anticipate potential risks associated with large-scale solar energy development in the region. Therefore, this study focuses on the effects of clouds on solar radiation in the framework of managing solar energy production in the region.

The climate of WA, which is controlled by the West African Monsoon, is typically characterized by an intense coverage of different cloud types [17,18] associated with a high spatial–temporal variability [19]. However, the impacts of these clouds on the incoming solar radiation needed for power generation are not very well studied in the region. Only a few studies (e.g., [11,20]) have tried to address this important issue due to the lack of surface observations, which are essential for any feasibility analysis concerning solar energy development in the region. However, these studies are limited to only a few locations where surface observations are available. As a result, a regional overview of the effects of clouds on the incoming solar radiation is lacking, leaving many open key questions concerning the long-term feasibility of regional-scale solar energy projects. Addressing some of these questions could help develop effective plans that would be crucial to managing the risks of integrating large shares of solar energy in the region. This could further help alleviate fears of massively investing in the development of the solar energy potential in the region. Thus, the goal of this study is to contribute to answering the following key questions:

- How does the sub-daily surface solar radiation vary from one year to the other in WA?
- What percentage of incoming solar radiation is attenuated by clouds in WA?
- How persistent are cloudy and cloudless conditions in the region?

The ambition is to provide relevant and usable information for stakeholders involved in the planning of solar energy projects in the region. For instance, the persistence of cloudiness at a location is

important in the siting and sizing of solar PV farms. Although WA is known to be cloudy, the persistence of cloudiness is still relatively unknown in many areas within the region, casting uncertainties regarding the feasibility of integrating large shares of solar PV power into the power systems. This important issue is addressed in this study in the context of solar energy production. Again, the estimation of the attenuation effect of clouds and the variability of solar radiation at several locations over WA (in different climatic zones) will provide an added value to previous studies (e.g., [11,21]) that focused on single locations. This approach could help develop specific plans tailored for managing solar energy production in different areas within the WA region. It is worth noting that dust has important effects on the incoming solar radiation, but we focus only on clouds in this study.

The article is organized as follows. Section 2 presents the dataset, study area, and methodology. Section 3 presents and discusses the findings of the study. In Section 4, we conclude and provide insights for the future.

## 2. Materials and Methods

### 2.1. Data

In this study, cloud cover and incoming surface solar radiation flux data are analyzed and the attenuation of the solar radiation by clouds is determined. The cloud cover and radiation data are extracted from the fifth generation of the state-of-the-art European Centre for Medium-range Weather Forecasts (ECMWF) Re-Analysis, which is also known as ERA5 (Detailed documentation at [22]. In [23], the ERA5 dataset was evaluated and used to analyze the synergies between renewable energy sources including solar energy in WA. The dataset is available at an hourly resolution with a horizontal resolution of $0.25° \times 0.25°$ on a regular grid. For this study, we analyzed only daytime hours for a 10-year period spanning from 2006 to 2015.

ERA5 provides 2D (and 3D) distributions of different cloud properties integrated for all levels within some predefined layers in the atmosphere. Here, we analyze the cloud fraction, which includes the total cloudiness (TC), low-level cloudiness (LLC), mid-level cloudiness (MLC), and high-level cloudiness (HLC). In the ERA5 dataset, TC, LLC, MLC, and HLC are clouds integrated from the surface to the top of the atmosphere (TOA), the surface to 800 hPa, 800 hPa to 450 hPa, and 450 hPa to TOA, respectively [24]. In addition to the cloud fraction, ERA5 provides the surface downwelling shortwave radiation fluxes in all-sky and clear-sky conditions. Table 1 provides a summary of all the input data used for this study.

**Table 1.** Summary of input data extracted from the European Centre for Medium-range Weather Forecasts ReAnalysis (ERA5) and used for this study.

| Input Data | Symbol | Details |
|---|---|---|
| Surface downwelling shortwave radiation, all sky | $SW^{\downarrow}$ | Input for cloud radiative attenuation of all clouds and of different cloud types |
| Surface downwelling shortwave radiation, clear sky | $SW^{\downarrow}_{CS}$ | |
| Total cloudiness | *TC* | Input for cloud radiative attenuation of all clouds |
| High-level cloudiness | *HLC* | Input for cloud radiative attenuation of high-level clouds |
| Mid-level cloudiness | *MLC* | Input for cloud radiative attenuation of mid-level clouds |
| Low-level cloudiness | *LLC* | Input for cloud radiative attenuation of low-level clouds |

Data Evaluation

A necessary condition for using the ERA5 dataset for such a study is to first evaluate its ability to reproduce the actual observations in the region of interest. In a recent study by [19] in WA, the ERA5 cloud fraction was compared with some synoptic in situ observations (and satellite data) from the region obtained from the Integrated Surface Database [25]. The comparison showed a satisfactory agreement between the reanalysis and in situ dataset (see Appendix S1 in [19]). Here, we evaluate the surface downwelling shortwave radiation flux with in situ observations in WA. For this, we use surface measurements from two sites of the AMMA-CATCH observatory (African Monsoon Multidisciplinary Analysis—Couplage de l'Atmosphère Tropicale et du Cycle eco-Hydrologique [26]). The two sites (red triangles in Figure 1) are located at Wankama South (2.6334° E and 13.6476° N) in Niger and Nalohou (1.6049° E and 9.7448° N) in Benin and provide complete surface solar radiation flux measurements for the period of study. Thus, solar radiation data from the closest grid points to the two sites in the ERA5 dataset are used for the evaluation complemented by the satellite-based Surface Radiation Data Set—Heliosat (SARAH) hourly solar irradiance time series [27], extracted from EUMETSAT Satellite Application Facility on Climate Monitoring (CM-SAF).

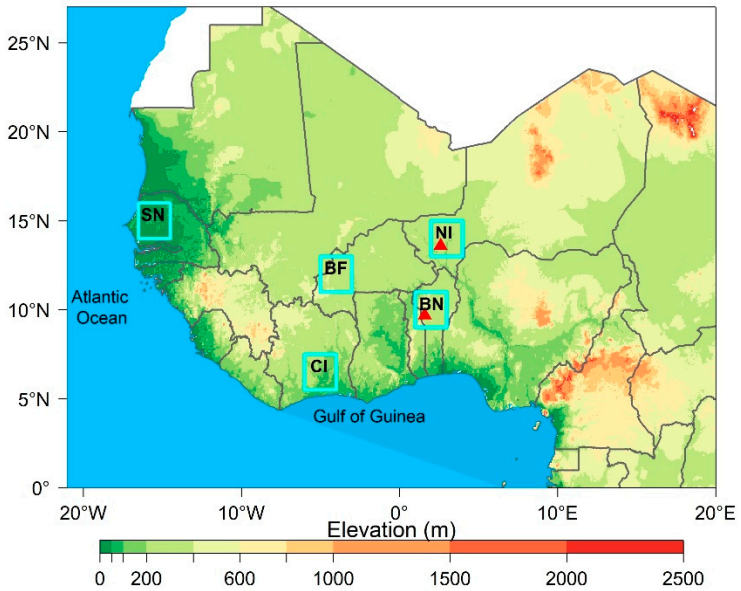


**Figure 1.** Elevation map of West Africa showing five 2° × 2° boxes across the region in Senegal (SN), Burkina Faso (BF), Niger (NI), Benin (BN, (and part of Togo)), and Cote d'Ivoire (CI). The map also shows the locations of the two AMMA-CATCH (African Monsoon Multidisciplinary Analysis—Couplage de l'Atmosphère Tropicale et du Cycle eco-Hydrologique) observatories in Benin and Niger (red triangles).

Figure 2 presents two Taylor diagrams showing the performance of ERA5 and SARAH in the evaluation with the surface observations in Benin and Niger, respectively. In Benin, ERA5 shows a good agreement with the surface observations with a correlation coefficient of about 0.92 and a root mean square error (RMSE) of 123 W $m^{-2}$. Likewise, in Niger, ERA5 shows a reasonable agreement with the surface observation with a correlation coefficient of about 0.84 and root mean square error of 182 W $m^{-2}$. In addition, in both stations, the ERA5 data exhibit similar scatter around the mean (standard deviation) as the observation.

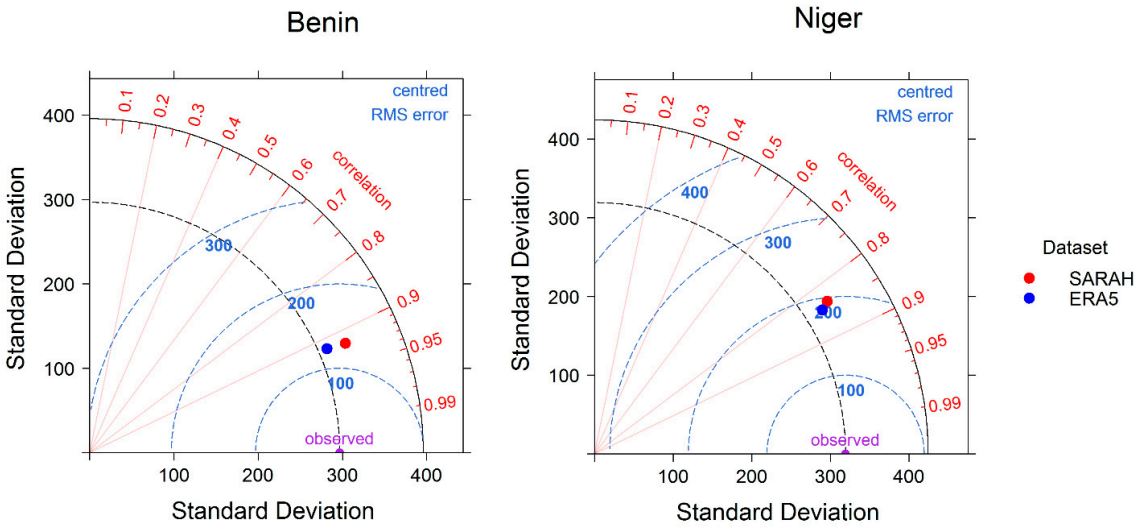


**Figure 2.** Taylor's diagrams showing the evaluation of ERA5 (and SARAH, or satellite-based Surface Radiation Data Set—Heliosat) with surface observations from the AMMA-CATCH observatories.

### 2.2. Methodology

The study domain is the whole of West Africa (Figure 1), but investigations are mainly performed over the five 2° × 2° bounded windows (light blue in Figure 1) across the WA region. These windows are located in different climatic and vegetation zones and their selection helps to provide a regional overview of cloud cover effects on the incoming solar radiation. Three of the windows are located in Senegal, Burkina Faso, and Niger, all in the Sahelian climate zone of WA [28]. The two other windows are located in Cote d'Ivoire and Benin in the Guinean and Sudanian climate zones of WA, respectively [29]. Additionally, all of these five windows are located in countries with plans for utility-scale solar energy development. The selection of the Niger and Benin windows is also motivated by the availability of complete surface observations used for the evaluation of the ERA5 data (Figure 2). Although the Senegal window is located in the Sahel region of WA, its proximity to the ocean (similar to the Cote d'Ivoire window) could lead to increased cloudiness compared to the other two Sahelian windows [30]. No window is located north of latitude 16° N, because this area is usually characterized by very low cloud coverage throughout the year [18,19].

To capture how the sub-daily surface solar radiation varies from one year to the other, the interannual variability of the hourly surface downwelling shortwave radiation flux, $SW^{\downarrow}$, is investigated with the coefficient of variation (CV) [31] over the five 2° × 2° windows in the WA region. The CV is unitless and is defined as the ratio of the standard deviation to the mean. In each window, the CV shows how the $SW^{\downarrow}$ measured for a given day and time varies across all years for the same day and time. Unlike the standard deviation, the interpretation of the CV is independent of the mean value or unit of measurement. Therefore, it is very suitable to compare the variability of the $SW^{\downarrow}$ from one window to the other and also within a particular window, the variability from one period (e.g., months and seasons) to the other.

Then, we analyze the occurrence and persistence of cloudy and cloudless sky conditions across the WA region. However, the impacts of the clouds on the incoming solar radiation have been determined over the five windows. To quantify the attenuation of incoming solar radiation by clouds at any given time $t$, we define the cloud shortwave radiation attenuation ($CRA^{\downarrow}_{SW}$). $CRA^{\downarrow}_{SW}$ refers to the quantity of incoming solar radiation that is lost through absorption or reflection (back to space) by clouds at any time. It is estimated by finding the difference between the $SW^{\downarrow}$ in $W\ m^{-2}$ and the clear-sky surface downwelling shortwave radiation flux, $SW^{\downarrow}_{CS}$ in $W\ m^{-2}$ [11,32]. $SW^{\downarrow}_{CS}$ is computed for the same atmospheric conditions of temperature, humidity, ozone, trace gases, and aerosols as the corresponding $SW^{\downarrow}$ (with clouds), but assuming that there are no clouds. Therefore, $CRA^{\downarrow}_{SW}$ only accounts for the

effects of clouds on the incoming solar radiation but not aerosols. To eliminate the influence of the time of the day and thus the solar elevation angle on the mean $CRA^{\downarrow}_{SW}$ value, we express the $CRA^{\downarrow}_{SW}$ at a given time as a percentage of the $SW^{\downarrow}_{CS}$ at that time. Thus,

$$CRA^{\downarrow}_{SW}(t) = \frac{SW^{\downarrow}_{CS}(t) - SW^{\downarrow}(t)}{SW^{\downarrow}_{CS}(t)} \times 100. \quad (1)$$

For each window, $CRA^{\downarrow}_{SW}$ is computed for all daytime hours from 06:00 UTC to 17:00 UTC at each grid point when clouds are present (i.e., when TC > 0) and the mean is determined. For each window, we assume that nearby areas will have similar characteristics in terms of the mean solar radiation received at the surface as well as its variability.

The computation of $CRA^{\downarrow}_{SW}$ considers the total cloudiness and does not differentiate the impacts of each cloud type (i.e., LLC, MLC, and HLC) on the incoming solar radiation. The impact of a particular cloud type can be determined following the same procedure and assumptions as Equation (1) but assuming only that cloud type is present, while the other cloud types are absent in the atmosphere. Thus, for each cloud type, we computed the associated $CRA^{\downarrow}_{SW}$ for periods during which only that cloud type was present i.e.,

$$CRA^{\downarrow}_{SW_{cloudtype}} = \begin{cases} CRA^{\downarrow}_{SW_{HLC}} \; if \; HLC > 0, \; MLC = 0, \; LLC = 0 \\ CRA^{\downarrow}_{SW_{MLC}} \; if \; MLC > 0, \; HLC = 0, \; LLC = 0 \\ CRA^{\downarrow}_{SW_{LLC}} \; if \; LLC > 0, \; HLC = 0, \; MLC = 0 \end{cases}. \quad (2)$$

From this, it is possible to determine the relationship between the coverage area (i.e., the cloud fraction) occupied by a given cloud type and its associated $CRA^{\downarrow}_{SW}$.

## 3. Results and Discussion

### *3.1. Variability of Received Surface Solar Radiation*

An important challenge for solar energy development is the intermittent nature of solar radiation mainly due to the high temporal variations in cloudiness leading to important fluctuations in solar power generation. This unfavorable situation is largely unavoidable at individual solar power plants, but robust planning can help to reduce the overall impact on the power grid. Knowledge of the short-term (e.g., one minute) variations of surface solar radiation at a given location is very important for the day-to-day management of the power grid. Estimating the variability of incoming solar radiation in WA at such short timescales may prove challenging given the lack of surface observations. Additionally, the hourly resolution of the ERA5 data makes it impossible to capture the intra-hour variability of surface solar radiation associated with cloud motion. Nevertheless, knowledge of a longer-term variability (e.g., month-to-month, season-to-season, year-to-year) is important for the successful integration of large shares of solar energy into the regional power systems. For this, it is necessary to understand how the solar radiation received at a specific place and time (hour, day, or month) varies from one year to the other. This could help characterize the uncertainty associated with the surface solar radiation received during different periods in a year.

Figure 3 shows the annual cycle of the CV computed from the interannual hourly surface solar radiation data over the 10 years for all the five selected windows. The cycle of the variability is similar in all the windows with a higher CV during the summer months in the core of the monsoon season and a lower CV during the driest months (ranging from November to May, depending on the region). This implies that the surface solar radiation received in the dry season does not change much from one year to the other, while there is a higher uncertainty during the summer months. This result is in agreement with results from other tropical regions where the most humid months are found to be associated with the largest variability of surface solar radiation (e.g., [33] in Brazil). Generally,

the variability appears to be higher in the southern part of WA where humidity is highest. For instance, during the core of the monsoon season, the variability is slightly higher in the Cote d'Ivoire and Benin windows compared to others. Moreover, in the dry months, the variability is highest in the windows that are close to the ocean (Cote d'Ivoire and Senegal). This result suggests that siting solar farms at humid locations in WA will present greater challenges and uncertainties mostly associated with fluctuations in power production. Thus, rigorous solutions such as the spatial diversification of PV farm sites [34] are required to alleviate the overall impacts of such challenges on the power grid.

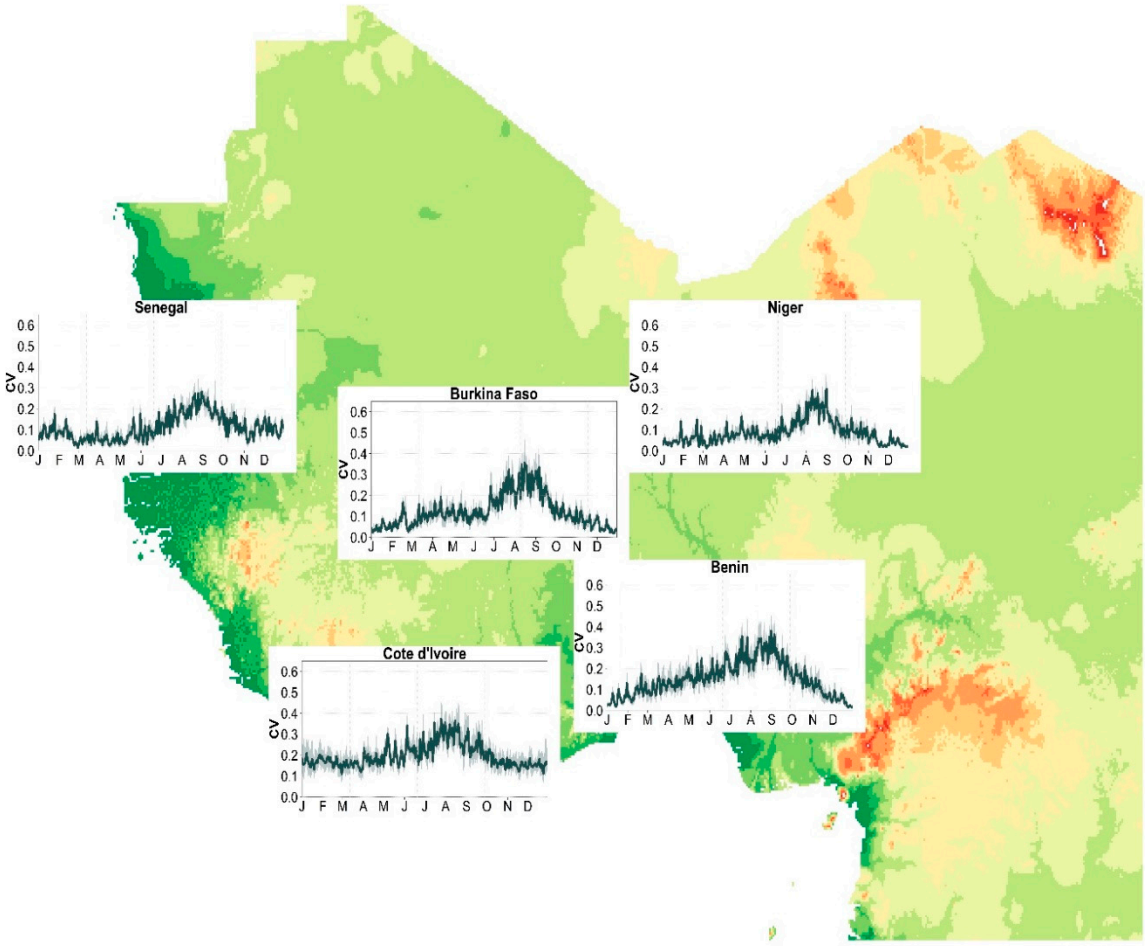


**Figure 3.** Annual cycle of coefficient of variation for the interannual hourly surface solar radiation received in West Africa.

### 3.2. Attenuation of Incoming Solar Radiation by Clouds

The mean annual evolution of the $CRA^{\downarrow}_{SW}$ (for total cloud cover) is shown in Figure 4. In all windows, the mean attenuation of incoming solar radiation by clouds (solid red curve) is highest in the summer from July to October, which corresponds to the core of the monsoon season in the region [35]. During this period, WA is characterized by moisture influx from the Guinean Gulf that increases cloud cover over the region, thus intensifying the attenuation of incoming solar radiation, which in turn will lead to a decrease in solar power generation. The maximum attenuation occurs in August when the Inter-Tropical Convergence Zone (ITCZ) is at its northernmost position in WA [36–38]. On the other hand, very low attenuations are observed from December to February when most of the WA region is characterized by dry weather conditions. This cycle of $CRA^{\downarrow}_{SW}$ follows the annual evolution of clouds in the region, as shown in available cloud climatologies (e.g., [19]).

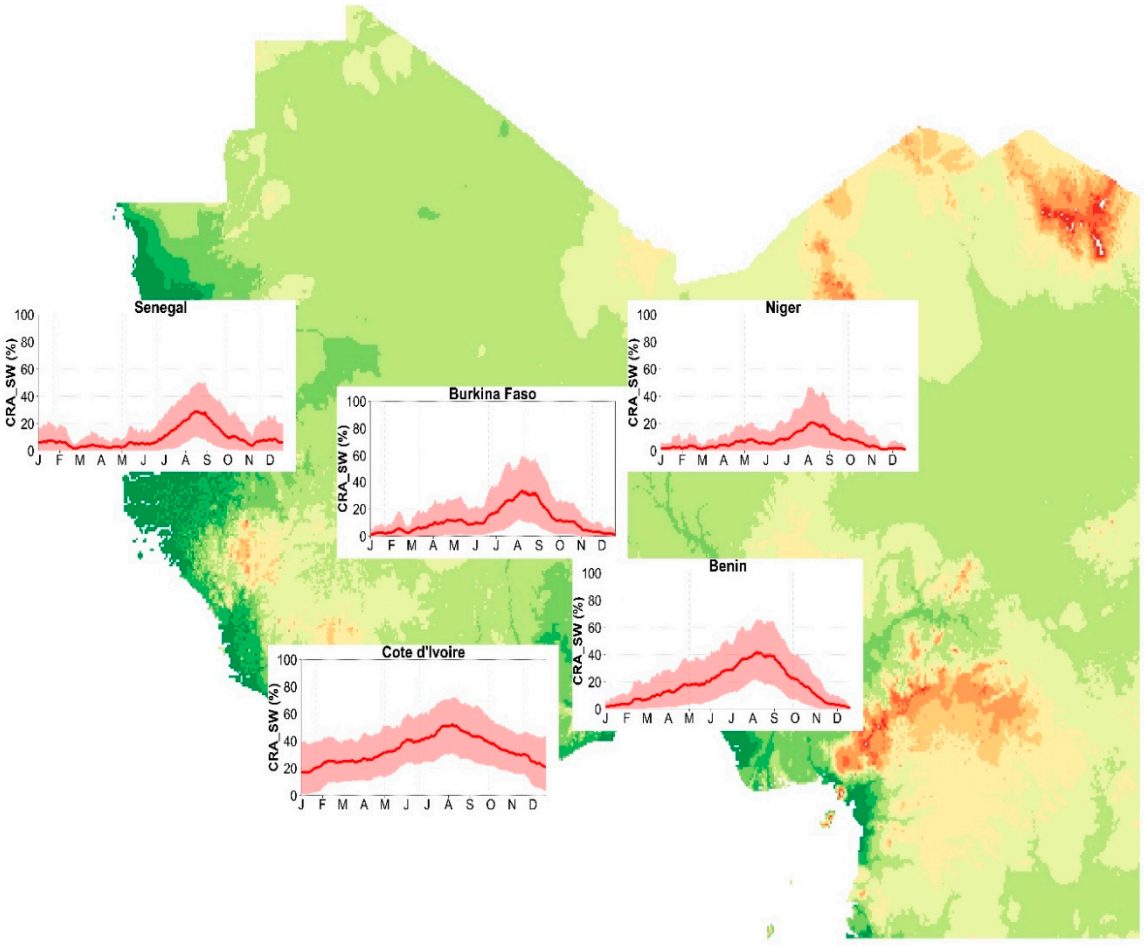


**Figure 4.** Mean annual cycle (solid curve) of cloud shortwave radiation attenuation in West Africa. Shaded regions are the 10th and 90th interpercentile range.

Although all the windows display similar annual cycles of $CRA_{SW}^{\downarrow}$, the attenuation of incoming solar radiation is highest in the southern part of WA. In all months, the mean $CRA_{SW}^{\downarrow}$ is higher in the Cote d'Ivoire and Benin windows compared to the other windows. In August, around 55% and 40% of incoming solar radiation are lost on average due to clouds in Cote d'Ivoire and Benin respectively compared to about 20%, 30%, and 35% in Niger, Senegal, and Burkina Faso. On the other hand, the mean attenuation is around 5% or less in all windows during January except in Cote d'Ivoire, where about 20% of the incoming solar radiation is lost. If we assume a $CRA_{SW}^{\downarrow}$ threshold of 30% as reasonable for exploiting the solar resource potential in WA, many areas could be considered suitable for siting solar power plants, as the mean $CRA_{SW}^{\downarrow}$ does not exceed this threshold in several months. In the Sahelian region, the mean $CRA_{SW}^{\downarrow}$ is rarely 30% or more except in August in Burkina Faso and Senegal. In the southern part of WA, the mean attenuation exceeds this arbitrary threshold value for longer periods i.e., from July to September in Benin and May to November in Cote d'Ivoire.

Furthermore, $CRA_{SW}^{\downarrow}$ in the summer months is associated with a large variability in all windows (shaded region representing the 10th and 90th interpercentile range). This could be due to a high degree of variation in the optical properties (such as cloud optical thickness) of the different cloud systems that occur over the region, but this needs to be investigated further. Thus, places such as Cote d'Ivoire and Benin with high mean $CRA_{SW}^{\downarrow}$ values exceeding the assumed threshold (especially in the summer) could have many other periods with lower attenuations. It is worth noting that in Cote d'Ivoire, the range of variability does not change throughout the year. However, in the other windows, the variability is mostly higher from June to September (April to June for Benin). Additionally, it is

important to highlight that the mean and variability of $CRA_{SW}^{\downarrow}$ in the Senegal window is not very different from the other Sahelian windows, regardless of its proximity to the Atlantic Ocean.

Figure 5 shows the mean seasonal evolution (from 2006 to 2015) of daily average surface downwelling shortwave radiation in clear-sky and cloudy conditions computed with ERA5. In the Northern Hemisphere, daylengths are longer (shorter) during the summer (winter), and thus, the radiation arriving at the top of the atmosphere is highest (lowest) during this period [39]. Thus, in a hypothetical scenario with no clouds in the atmosphere, the incoming solar radiation over WA will be highest in the summer months from March to May (MAM) and June to August (JJA) and lowest from December to February (DJF) and September to November (SON), as shown in Figure 5a. However, in the southern part of WA, the frequent occurrence of thick multi-layered clouds [40] responsible for the high $CRA_{SW}^{\downarrow}$ values severely reduces the incoming solar radiation during the summer months (JJA in Figure 5b). On the other hand, although the attenuation of incoming solar radiation in the Sahel and north of WA (north of latitude 10° N) is larger during the summer months, maximum solar radiation is received during this period. This is due to the relatively lower coverage of clouds in the Sahel, as shown by [18,19]. Again, most clouds occurring in the Sahelian region are thin [41] (mid- and high-level clouds); thus, their total impact on the incoming shortwave radiation is relatively low. Moreover, daylengths are longer at higher latitudes during the summer and thus, the Sahel receives more solar radiation. During DJF, the amount of solar radiation received over the Sahel region with or without clouds in the atmosphere is similar. The reason for this is that cloud coverage in DJF is extremely low over this area.

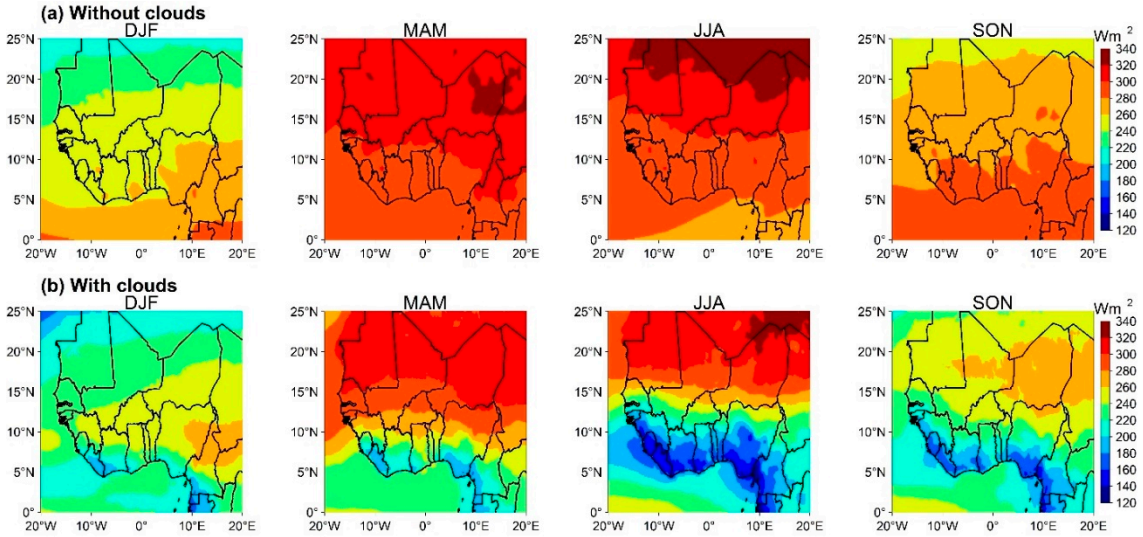


**Figure 5.** Mean seasonal evolution (2006 to 2015) of daily average surface downwelling shortwave radiation in (**a**) clear-sky and (**b**) cloudy conditions computed with ERA5. DJF refers to the December–January–February period, MAM refers to March–April–May, JJA refers to June–July–August, and SON refers to September–October–November.

In terms of cloudiness, the most challenging period to manage a power grid integrated with solar energy in WA is the summer period due to high $CRA_{SW}^{\downarrow}$ values and the associated variance (Figure 4). With a similar variance of $CRA_{SW}^{\downarrow}$ across all windows (±20% as shown in Figure 4) during the summer months, the difficulty in the management will be the same over the whole region, even though the Sahel and north of WA receives more solar radiation than the south (Figure 5). On the other hand, the variance in the other months is rather low in all windows except in Cote d'Ivoire, which has high variance throughout the entire year. The high mean values and variance of $CRA_{SW}^{\downarrow}$ in Cote d'Ivoire are likely due to the all-year-long presence of LLCs in this area of WA, as shown by [42]. Theoretically, this will make the management of solar energy production and power grid even more difficult in Cote

d'Ivoire and its environs (southern WA). Thus, the PV farms in this region will have to be oversized to reduce the impacts of the uncertainty in power production due to the high variability of $CRA^{\downarrow}_{SW}$ throughout the year. Nevertheless, even though the variance in other months is low in the other windows (especially in the Sahel windows), higher temperatures during those months [28] could also reduce the conversion efficiency of the PV cells. In a nutshell, cloudiness should not be a blocking factor for investing in solar energy in southern WA, but there is a need to consider all of this information in the operational daily management and seasonal planning of solar power generation over the entire WA region.

### *3.3. Dependence of Cloud Radiation Attenuation of Cloud Fraction*

So far, we have only shown the impact of total cloud coverage on the attenuation of incoming solar radiation. However, differences in microphysical properties mean that $CRA^{\downarrow}_{SW}$ differs across cloud types [14]. Macrophysical properties of clouds such as cloud fraction could also have a significant influence on the radiative effect clouds, but this is often overlooked. Thus, the emphasis in this study is not to provide the $CRA^{\downarrow}_{SW}$ caused by each of the three cloud types but rather to determine the relationship between the fractional coverage of each cloud type and its associated $CRA^{\downarrow}_{SW}$. The correlation coefficient ($R$) between cloud fraction and $CRA^{\downarrow}_{SW}$ for each cloud type is presented in Table 2. In all the five selected windows, $CRA^{\downarrow}_{SW}$ shows a strong dependence on the cloud fractional coverage for LLCs and MLCs. Thus, a larger (smaller) fraction of LLC or MLC results in a higher (lower) attenuation of the incoming solar radiation. As shown by [19], during JJA, the fractional coverage of LLC and MLC intensifies over southern WA, especially near the coastal areas. This leads to the high mean $CRA^{\downarrow}_{SW}$ in the summer (Figure 4) and explains the low values of surface solar radiation around this area in JJA (Figure 5b). On the contrary, the dependence of $CRA^{\downarrow}_{SW}$ on cloud fractional coverage is relatively weaker for HLCs. This is likely due to the optically thin nature of HLCs, which allows a large proportion of incoming solar radiation to pass through with very low attenuation. [14] showed that given representative environmental conditions for the same liquid water path and ice water path, clouds containing only liquid particles have larger optical depths and thus higher solar albedo effects. It was revealed in the same study that clouds that are composed entirely of water particles have a higher solar albedo effect due to the large liquid water paths. HLCs consist mostly of ice particles, while MLCs and LLCs are largely composed of liquid water particles, which explains why the $CRA^{\downarrow}_{SW}$ of HLCs does not show a strong relationship with the fractional coverage.

**Table 2.** Relationship between cloud fraction and cloud shortwave radiation attenuation for the different cloud types in the five selected windows.

| Region | $R\left(CRA^{\downarrow}_{SW}\right.$ vs. Cloud Fraction$\left.\right)$ | | |
|---|---|---|---|
| | HLC | MLC | LLC |
| Senegal | 0.59 | 0.94 | 0.93 |
| Burkina Faso | 0.53 | 0.93 | 0.99 |
| Niger | 0.5 | 0.92 | 0.91 |
| Benin | 0.45 | 0.93 | 0.96 |
| Cote d'Ivoire | 0.72 | 0.97 | 0.92 |

### *3.4. Multi-Timescale Persistence of Sky Conditions*

Given the strong positive relationship between cloud fraction and $CRA^{\downarrow}_{SW}$ for LLCs and MLCs, we analyze their occurrence and persistence within a given temporal window to qualitatively infer the reliability of solar power generation from solar plants in the region. As shown by [11], these LLCs and MLCs are associated with high attenuation effects on incoming solar radiation in WA. Taking this into account together with the dependence of the attenuation on the fractional coverage of these cloud

types, we can assume that a significant amount of the incoming solar radiation will be lost when a large fraction of the sky is covered by LLCs and/or MLCs. Figure 6 shows the annual mean occurrence frequency of LLCs, MLCs, and cloudless sky conditions that persist for a few to several hours during the daytime. Only LLCs and MLCs with high coverage in the sky (at least 50%) are considered here.

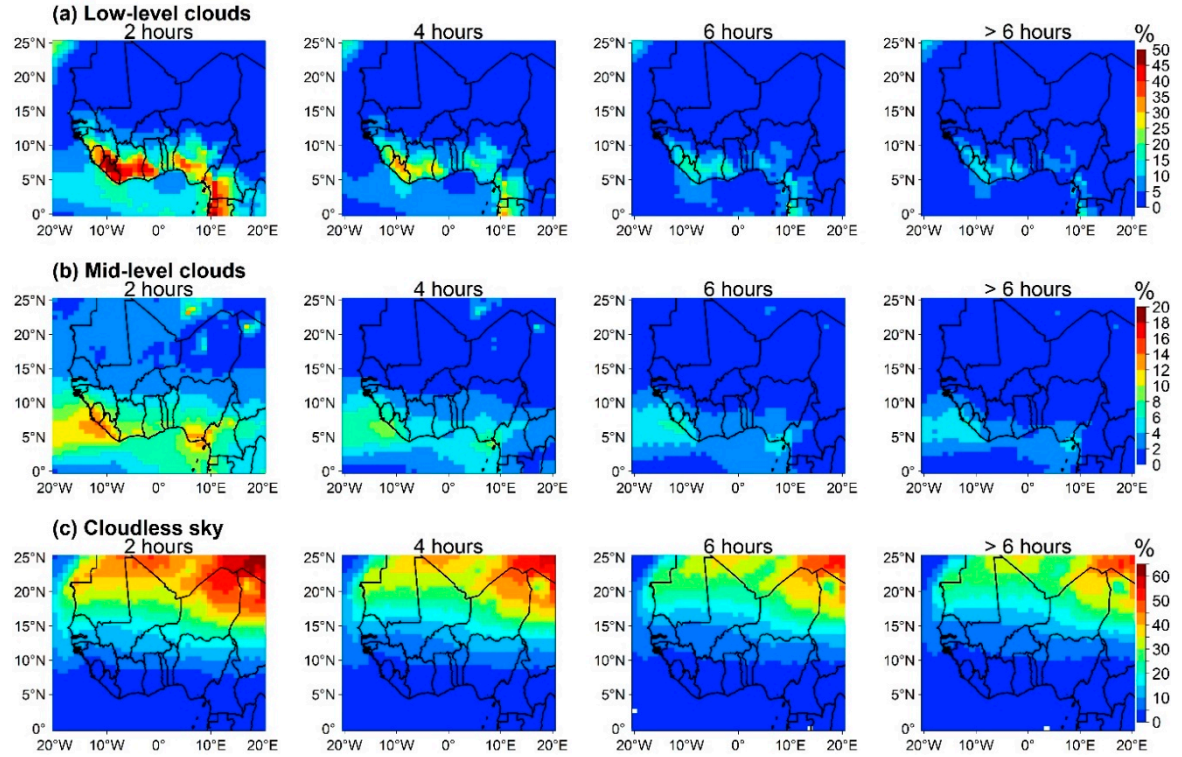


**Figure 6.** Spatial distribution of the occurrence frequency of (**a**) low-level cloudiness (LLC), (**b**) mid-level cloudiness (MLC), and (**c**) cloudless sky conditions that persist for multiple hours in West Africa. Only LLC and MLC occurrences with at least 50% coverage are considered.

In general, there is a high occurrence frequency for LLCs (Figure 6a) and MLCs (Figure 6b) that persist for at least two consecutive hours in the southern part of WA (south of latitude 10° N), especially around the coastal areas. LLCs persist for exactly two consecutive hours from 30% to 50% of the time in an average year. Over these same regions, LLC occurrence can persist for several consecutive hours (more than 2 h) during a significant number of times in a year. This includes about 5% to 15% extreme cases during which LLCs can persist for more than six consecutive hours. This means that for about 18 to 55 days in an average year, the received surface solar radiation will likely be well below the expected average for at least more than half of the time during each day. In the same way, MLCs can persist for exactly two consecutive hours during about 8% to 16% of the time in an average year. MLCs can also persist for several consecutive hours (more than 2) for a lot of days in a given year. For example, in Liberia and Sierra Leone as well as the southern parts of Cote d'Ivoire, Ghana, and Nigeria, MLCs can persist for more than six consecutive hours during 2% to 6% of the year (about 7 to 22 days). Thus, solar power generation could be severely disrupted during those periods over southern WA.

The Sahelian and northern parts of WA (north of latitude 10° N) are characterized by a high occurrence frequency of cloudless sky conditions (Figure 6c). Without clouds in the atmosphere, only a small fraction of the incoming solar radiation will be attenuated due to other atmospheric constituents (water vapor, trace gases, ozone, etc.). This is an ideal case for solar PV farm managers, as the solar PV panels receive maximum solar radiation to produce energy. For instance, over the northern parts of Niger, Mali, and Mauritania, cloudless sky conditions can persist for more than six consecutive hours during about 30% of the time in an average year. However, these areas are characterized by a

high concentration of dust particles [43,44], which could severely reduce the incoming solar radiation. However, this issue of dust influence on incoming solar radiation is not addressed in this study.

For solar energy management, it is also relevant to show the distribution of these persistent conditions in seasons or months. Figure 7 shows the mean occurrence frequency of persistent LLCs, MLCs, and cloudless sky conditions in the five selected windows for each season. Due to the steep spatial gradient of the occurrence frequency of cloudy and cloudless condition between the north and south of WA, the range of the $y$-axis differs across the chosen region: up to 20% for the three Sahelian windows, 30% for Benin, and 60% for Cote d'Ivoire. In general, the persistence of cloudiness in all seasons seems to decrease with latitude except for the Senegal window, which is situated at a higher latitude than the Niger window, yet has a relatively higher frequency of persistent LLCs and MLCs. This is likely due to the proximity of Senegal to the Atlantic Ocean, which leads to an intrusion of cold moist westerly winds enhancing cloud formation and occurrence in this area. This enhanced cloud formation could explain the relatively higher $CRA_{SW}^{\downarrow}$ during the rainy season in Senegal than Niger.

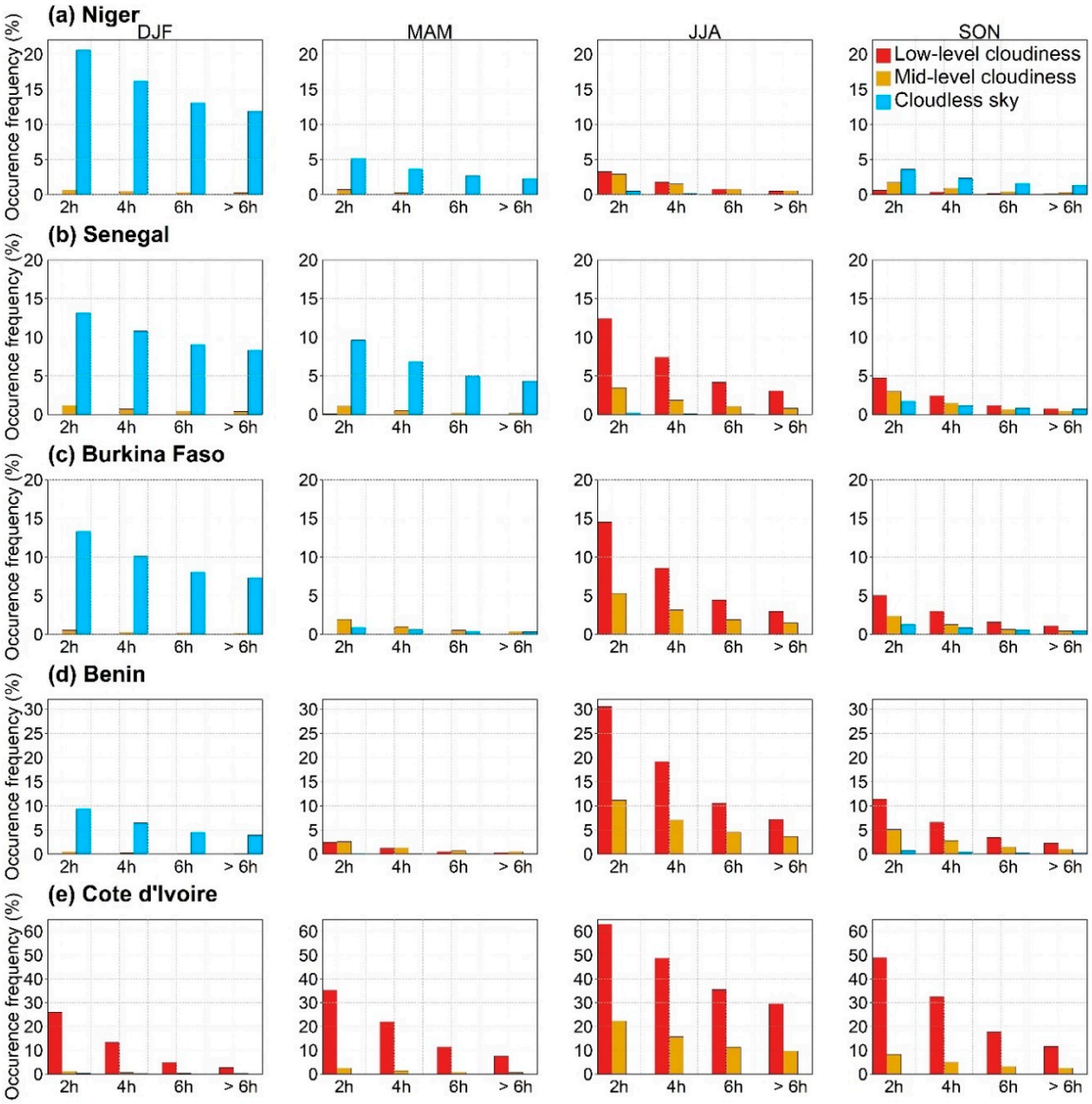


**Figure 7.** Seasonal mean occurrence frequency of low-level cloudiness (LLC), mid-level cloudiness (MLC), and cloudless sky conditions that persist for multiple hours in (**a**) Niger, (**b**) Senegal, (**c**) Burkina Faso, (**d**) Benin and (**e**) Cote d'Ivoire. Only LLC and MLC occurrences with at least 50% coverage are considered. Note the differences in the range of the $y$-axis for the different regions.

In the three Sahel windows, the occurrence of persistent LLCs and MLCs are usually limited to JJA and SON (not in Niger). They are most frequent in JJA, with a mean occurrence frequency for LLCs (MLCs) that occur for exactly two hours, around 12.5% (4%), 14.5% (5.5), and 3.5% (3%) in Senegal, Burkina Faso, and Niger, respectively. The occurrence frequency of LLCs that persist for more than six hours is about 3% in JJA in both Senegal and Burkina Faso. Persistent cloudless sky conditions, on the other hand, are spread across all seasons except in JJA. Their occurrence is high in DJF and MAM (not in Burkina Faso). In Cote d'Ivoire, on the other hand, persistent LLCs are spread across all seasons (highest in JJA), while persistent MLCs occur mostly in JJA and SON. In Benin, the persistent LLCs and MLCs mostly occur in JJA and SON (and there are few occurrences in MAM). The occurrence of persistent cloudless sky conditions is rare in Cote d'Ivoire during all seasons, while they occur only during DJF in Benin. The implication for the all-year-long spread of persistent LLCs and MLCs (in JJA and SON) in Cote d'Ivoire is that disruptions in solar power generation can happen anytime during the year and can persist for longer durations. Thus, emergency backup power sources are needed at all times. In the other windows, disruptions in solar power generation are likely to occur for relatively short periods (i.e., mostly in JJA).

During overcast conditions, when the entire view of the sky is covered by one cloud type or a mix of cloud types, significant amounts of incoming solar radiation could be lost. The occurrence of persistent overcast conditions is very low over parts of the Sahel region and high over southern WA (not shown). Nevertheless, several hours of overcast weather do not necessarily imply significant losses of the incoming solar radiation. For instance, overcast conditions of only HLCs will not lead to significant losses of the incoming solar radiation due to the optically thin nature of such clouds and the associated low attenuation effects, as shown by [11]. However, overcast conditions of LLCs and/or MLCs could reduce a large portion of the incoming solar radiation available for solar power generation. Thus, the occurrence frequency of such overcast conditions is to be interpreted with caution.

For the overall management of the PV plant, it is also necessary to characterize the received surface solar radiation (as usable or non-usable) and the persistence associated with each category. Here, we divide the received surface solar radiation into three classes, namely: Low ($SW^{\downarrow} < 100$), Moderate ($100 \leq SW^{\downarrow} \leq 500$), and High ($SW^{\downarrow} > 500$). It should be noted that the thresholds associated with the three categories are arbitrarily chosen. With a single PV panel, the category of 'Low' SW will lead to a very low power production, which may be considered *non-usable*, while the other categories will lead to relatively higher productions. However, in a large solar farm with several hundreds of PV panels, the collective power output when the solar radiation class is 'Low' can still be significant (provided $SW^{\downarrow}$ is not zero). Figure 8 shows the seasonal occurrence frequency of persistent 'Low', 'Moderate', and 'High' available surface solar radiation for the Niger, Benin, and Cote d'Ivoire windows in the Sahel, Savannah, and Guinean vegetation zones of WA, respectively. The results for the Senegal and Burkina Faso windows are not shown, because they are similar to those obtained for Niger.

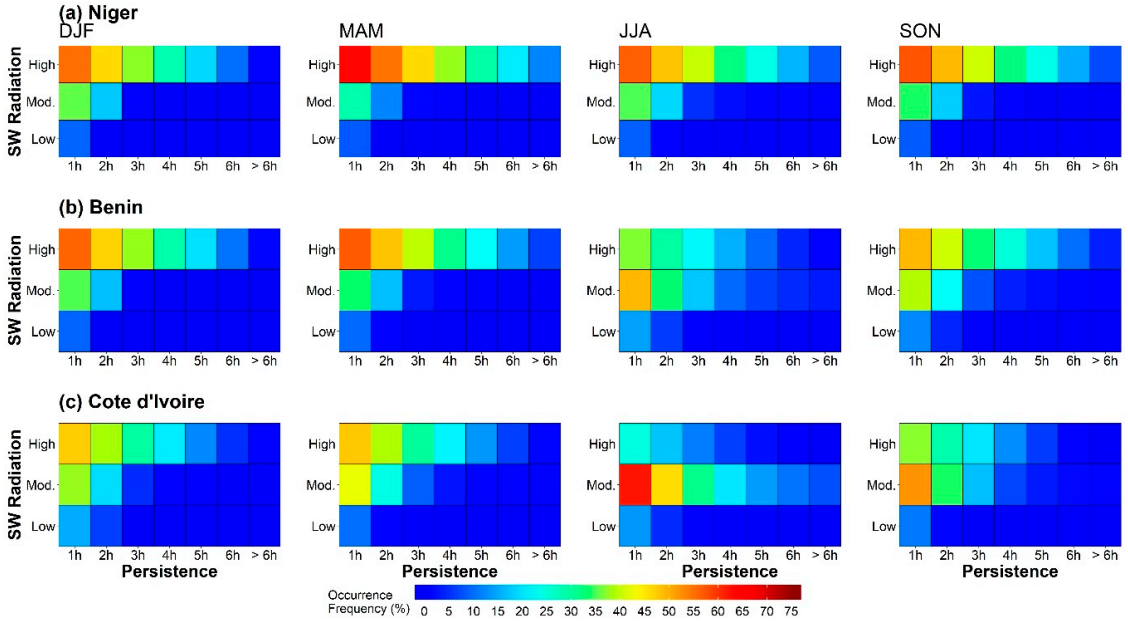


**Figure 8.** Seasonal mean occurrence frequency of Low ($SW^{\downarrow} < 100$), Moderate ($100 \leq SW^{\downarrow} \leq 500$), and High ($SW^{\downarrow} > 500$), received surface irradiance that persist for multiple hours in the (**a**) Niger, (**b**) Benin, and (**c**) Cote d'Ivoire windows for all seasons.

In all the windows, there are very few occurrences of persistent events of 'Low' $SW^{\downarrow}$ in all seasons. On the other hand, persistent 'Moderate' and 'High' $SW^{\downarrow}$ events are more frequent in all seasons. Persistent 'High' $SW^{\downarrow}$ dominates in Niger and Benin in all seasons. For example, during JJA in Niger, the 'High' $SW^{\downarrow}$ can persist up to three consecutive hours for about 45% of the time. Similarly, during DJF and MAM in Cote d'Ivoire, persistent 'High' $SW^{\downarrow}$ are more frequent. However, persistent 'Moderate' $SW^{\downarrow}$ events dominate during JJA in Cote d'Ivoire, which is likely a result of the intensification of cloud coverage over the area during this period. Therefore, solar power production during JJA in Cote d'Ivoire is expected to be moderate for prolonged periods. Thus, power plants in this area will need to be oversized to compensate for the reduced productions. It is interesting to see that the frequency of persistent 'Low' $SW^{\downarrow}$ events in Cote d'Ivoire is very low in all seasons, regardless of the intense cloud coverage in the southern part of WA. Consequently, extremely low solar power production will not linger for long periods. This is also true for all the other areas considered in the study, as shown in Figure 8.

Generally, the high frequency of persistent 'High' $SW^{\downarrow}$ events found in all windows (except JJA in Cote d'Ivoire) could be considered as favorable for solar energy development in the region. For solar power production, this result can be interpreted in different ways, depending on the type and size (capacity) of the PV plant. For small-scale off-grid PV power systems without battery storage, certain tasks that may require up to a given number of hours (e.g., 3 h) of power supply (such as water pumping in a household or office building) can be performed frequently during the season. Some of these tasks (e.g., water pumping) are not performed every day, and so it is necessary to schedule periods when they will be performed. This scheduling activity may require also understanding the spread of such persistent events of 'High' $SW^{\downarrow}$ during the season. However, this is beyond the scope of this study but needs to be investigated. On the other hand, for large-scale PV power plants (off-grid or grid-connected), persistent 'High' $SW^{\downarrow}$ events may lead to excess power production, especially during off-peak hours. This excess electricity will be lost unless there is a storage facility (e.g., battery) to temporarily store the excess energy produced and released when needed.

## 4. Summary and Conclusions

In this paper, we used the state-of-the-art ERA5 reanalysis dataset to show the occurrence of cloud cover in WA and assess its impacts on surface solar radiation in the context of planned large-scale solar energy generation in the region. The goal was to contribute to answering some key relevant questions to provide useful information for stakeholders involved in the planning of large-scale solar energy projects in the region.

The results showed that the attenuation of incoming solar radiation by cloud cover is strongest in the summer months during the core of the monsoon season in all parts of WA. Analysis of the year-to-year variability of the surface solar radiation also revealed a higher uncertainty in the received solar radiation during the summer (wetter) months as compared to the drier months. The southern part of WA is characterized by a much stronger attenuation of incoming solar radiation due to intense cloudiness as well as a relatively higher uncertainty in the summertime surface solar radiation. However, this does not necessarily imply that southern WA is not suitable for siting solar power plants, as there is still enough solar radiation received over this region, as shown in Figure 5b and in previous studies (e.g., [5]). However, it is necessary to develop robust plans to successfully integrate solar energy in the power grid of countries across the region, such as identifying synergies with other renewable sources and developing reliable backup sources to increase the flexibility of power systems. Indeed, many countries across the world receive lower solar radiation but still have successfully running solar power plants (e.g., in Europe [45]).

We also showed that cloudy conditions can persist for several hours over southern WA, thus reducing the incoming solar radiation for a significant period. In contrast, cloudless weather conditions occur frequently in the northern part of WA. However, this result is to be interpreted with caution. Firstly, the 1-h resolution of the ERA5 data could lead to uncertainty in the analysis of cloud persistence as clouds can vary at much shorter timescales (e.g., a few minutes). Again, even though there is a high occurrence frequency of persistent cloudless conditions in northern WA, this region is associated with high amounts of dust particles, which also have important attenuation effects on the incoming solar radiation. In addition, high temperatures in northern WA may reduce the conversion efficiency of PV cells.

Due to the lack of surface observations in the region, reanalysis and satellite-derived products provide a viable alternative to assess solar energy feasibility in the future. However, it is important to note that the reanalysis data used in this study have some biases over the study region, as shown by [19] and in Section 2.1, although it also presents satisfactory agreement with surface observations. Satellite products are also associated with some uncertainties. For example, as shown by [18], large differences exist between different satellite products over the WA region. Again, passive geostationary satellites, which usually have a high temporal resolution, have difficulty in detecting low-lying clouds when there are overlying upper-level clouds, which in turn affects shortwave radiation estimates. Most active satellite sensors that are less prone to this issue also lack continuity, which may lead to large uncertainties. Hence, an integrated assessment with different data products may help mitigate such uncertainties in future studies.

This study provides important climate information with a regional overview for stakeholders involved in the planning of large-scale and long-term renewable energy projects in WA. It also provides a blueprint for carrying out future analysis, ideally with a higher resolution dataset, which is needed to address the feasibility of solar energy development in the region. An important extension of this work would be to consider the decadal fluctuations of solar irradiance, which was not considered in this study, since only 10 years of data were used. This may be important to assess the long-term feasibility of solar energy projects in the region, and it needs to be investigated. Again, it could be useful to assess the combined effect of both clouds and dust on the incoming solar radiation as well as to distinguish between the spatiotemporal radiative effects of both parameters.

**Author Contributions:** The study framework was conceived by D.K.D., S.A., and A.D.; D.K.D. performed all calculations and visualization and drafted the original manuscript. D.K.D., S.A., and A.D. analyzed and discussed the results. R.A. contributed to the answers to reviewers and editing of the revised manuscript. All authors have read and agreed to the published version of the manuscript.

**Funding:** The research leading to this publication has been supported by the French National Research Institute for Sustainable Development IRD (Institut de Recherche pour le Développement, France).

**Acknowledgments:** We thank ECMWF for providing ERA5 reanalysis. We wish to express our gratitude to the AMMA-CATCH DB for providing surface observations used for data evaluation. We are also grateful to the Institute of Environmental Geosciences (IGE; University of Grenoble—Alpes, France) and to the Laboratoire de Physique de l'Atmosphère et de Mécanique des Fluides (LAPA-MF; University Felix Houphouet Boigny, Côte d'Ivoire) who hosted DKD during his stay in Grenoble and Abidjan in the framework of the International joint laboratory NEXUS on climate, water, land, energy and climate services (LMI NEXUS). Finally, we thank all the four anonymous reviewers whose comments and suggestions helped to improve this article.

**Conflicts of Interest:** The authors declare no conflict of interest.

## References

1. IPCC. *Climate Change 2013: The Physical Science Basis. Contribution of Working Group I to the Fifth Assessment Report of the Intergovernmental Panel on Climate Change*; Stocker, T.F., Qin, D., Plattner, G.-K., Tignor, M., Allen, S.K., Boschung, J., Nauels, A., Xia, Y., Bex, V., Midgley, P.M., Eds.; Cambridge University Press: Cambridge, UK; New York, NY, USA, 2013. [CrossRef]
2. Allen, M.R.; Dube, O.P.; Solecki, W.; Aragón-Durand, F.; Cramer, W.; Humphreys, S.; Kainuma, M.; Kala, J.; Mahowald, N.; Mulugetta, Y.; et al. Framing and Context. In *Global Warming of 1.5 °C. An IPCC Special Report on the Impacts of Global Warming of 1.5 °C Above Pre-Industrial Levels and Related Global Greenhouse Gas Emission Pathways, In the Context of Strengthening the Global Response to the Threat of Climate Change*; Masson-Delmotte, V., Zhai, P., Pörtner, H.-O., Roberts, D., Skea, J., Shukla, P.R., Pirani, A., Moufouma-Okia, W., Péan, C., Pidcock, R., et al., Eds.; IPCC: Geneva, Switzerland, 2018.
3. *Global Energy & $CO^2$ Status Report 2019*; IEA: Paris, France, 2019.
4. Rogelj, J.; Shindell, D.; Jiang, K.; Fifita, S.; Forster, P.; Ginzburg, V.; Handa, C.; Kheshgi, H.; Kobayashi, S.; Kriegler, E.; et al. Mitigation Pathways Compatible with 1.5 °C in the Context of Sustainable Development. In *Global Warming of 1.5 °C. An IPCC Special Report on the Impacts of Global Warming of 1.5 °C Above Pre-Industrial Levels and Related Global Greenhouse Gas Emission Pathways, in the Context of Strengthening the Global Response to the Threat of Climate Change*; Masson-Delmotte, V., Zhai, P., Pörtner, H.-O., Roberts, D., Skea, J., Shukla, P.R., Pirani, A., Moufouma-Okia, W., Péan, C., Pidcock, R., et al., Eds.; IPCC: Geneva, Switzerland, 2018.
5. Yushchenko, A.; de Bono, A.; Chatenoux, B.; Patel, M.K.; Ray, N. GIS-Based Assessment of Photovoltaic (PV) and Concentrated Solar Power (CSP) Generation Potential in West Africa. *Renew. Sustain. Energy Rev.* **2017**, *81*, 2088–2103. [CrossRef]
6. Hermann, S.; Miketa, A.; Fichaux, N. *Estimating the Renewable Energy Potential in Africa: A GIS-Based Approach*; IRENA-KTH working paper; International Renewable Energy Agency: Abu Dhabi, UAE, 2014.
7. MPEER (Ministre du Pétrole, de l'Energie et des E. R). Rapport d'Activités MPEER 2018. Available online: http://www.energie.gouv.ci/uploads/documents/rapports/RAPPORT_D_ACTIVITES_MPEER_2018.pdf (accessed on 5 August 2020).
8. Kuwonu, F. Harvesting the Sun. Scaling Up Solar Power to Meet Africa's Energy Needs. Available online: https://www.un.org/africarenewal/magazine/april-2016/harvesting-sun (accessed on 15 May 2020).
9. Moner-Girona, M.; Bódis, K.; Korgo, B.; Huld, T.; Kougias, I.; Pinedo-Pascua, I.; Monforti-Ferrario, F.; Szabó, S. *Mapping the Least-Cost Option for Rural Electrification in Burkina Faso: Scaling-up Renewable Energies*; Publications Office of the European Union: Luxembourg, 2017. [CrossRef]
10. Pyrina, M.; Hatzianastassiou, N.; Matsoukas, C.; Fotiadi, A.; Papadimas, C.D.; Pavlakis, K.G.; Vardavas, I. Cloud Effects on the Solar and Thermal Radiation Budgets of the Mediterranean Basin. *Atmos. Res.* **2013**, *152*, 14–28. [CrossRef]
11. Bouniol, D.; Couvreux, F.; Kamsu-Tamo, P.H.; Leplay, M.; Guichard, F.; Favot, F.; O'connor, E.J. Diurnal and Seasonal Cycles of Cloud Occurrences, Types, and Radiative Impact over West Africa. *J. Appl. Meteorol. Climatol.* **2012**, *51*, 534–553. [CrossRef]

12. Dajuma, A.; Yahaya, S.; Touré, S.; Diedhiou, A.; Adamou, R.; Konaré, A.; Sido, M.; Golba, M. Sensitivity of Solar Photovoltaic Panel Efficiency to Weather and Dust over West Africa: Comparative Experimental Study between Niamey (Niger) and Abidjan (Côte d'Ivoire). *Comput. Water Energy Environ. Eng.* **2016**, *5*, 123–147. [CrossRef]
13. Stanelle, T.; Vogel, B.; Vogel, H.; Bäumer, D.; Kottmeier, C. Feedback between Dust Particles and Atmospheric Processes over West Africa during Dust Episodes in March 2006 and June 2007. *Atmos. Chem. Phys.* **2010**, *10*, 10771–10788. [CrossRef]
14. Liou, K.N. *An Introduction to Atmospheric Radiation Volume 84 of International Geophysics*, 2nd ed.; Elsevier Science: Amsterdam, The Netherlands, 2002.
15. Wang, K.C.; Dickinson, R.E.; Wild, M.; Liang, S. Atmospheric Impacts on Climatic Variability of Surface Incident Solar Radiation. *Atmos. Chem. Phys.* **2012**, *12*, 9581–9592. [CrossRef]
16. Engeland, K.; Borga, M.; Creutin, J.-D.; François, B.; Ramos, M.-H.; Vidal, J.-P. Space-Time Variability of Climate Variables and Intermittent Renewable Electricity Production–A Review. *Renew. Sustain. Energy Rev.* **2017**, *79*, 600–617. [CrossRef]
17. van der Linden, R.; Fink, A.H.; Redl, R. Satellite-Based Climatology of Low-Level Continental Clouds in Southern West Africa during the Summer Monsoon Season. *J. Geophys. Res. Atmos.* **2015**, *120*, 1186–1201. [CrossRef]
18. Hill, P.G.; Allan, R.P.; Chiu, J.C.; Stein, T.H.M. A Multisatellite Climatology of Clouds, Radiation, and Precipitation in Southern West Africa and Comparison to Climate Models. *J. Geophys. Res.* **2016**, *121*, 10857–10879. [CrossRef]
19. Danso, D.K.; Anquetin, S.; Diedhiou, A.; Lavaysse, C.; Kobea, A.; Touré, N.E. Spatio-Temporal Variability of Cloud Cover Types in West Africa with Satellite-Based and Reanalysis Data. *Q. J. R. Meteorol. Soc.* **2019**, *145*, 3715–3731. [CrossRef]
20. Bonkaney, A.; Madougou, S.; Adamou, R. Impacts of Cloud Cover and Dust on the Performance of Photovoltaic Module in Niamey. *J. Renew. Energy* **2017**, *2017*, 8. [CrossRef]
21. Hill, P.G.; Allan, R.P.; Chiu, J.C.; Bodas-Salcedo, A.; Knippertz, P. Quantifying the Contribution of Different Cloud Types to the Radiation Budget in Southern West Africa. *J. Clim.* **2018**, *31*, 5273–5291. [CrossRef]
22. Copernicicus Climate Change Service (C3S). ERA5: Fifth Generation of ECMWF Atmospheric Reanalysis of the Global Climate; Copernicus Climate Change Service Climate Data Store (CDS). Available online: https://cds.climate.copernicus.eu/cdsapp#!/home (accessed on 5 September 2018).
23. Sterl, S.; Liersch, S.; Koch, H.; Lipzig, N.P.M.V.; Thiery, W. A New Approach for Assessing Synergies of Solar and Wind Power: Implications for West Africa. *Environ. Res. Lett.* **2018**, *13*. [CrossRef]
24. Forbes, R. Clouds and Precipitation: From Models to Forecasting. Available online: https://confluence.ecmwf.int/download/attachments/70951731/cloud_forbes_TCOP_Feb2017.pdf?api=v2 (accessed on 5 August 2020).
25. Lott, N.; Baldwin, R.; Jones, P. The FCC Integrated Surface Hourly Database, a New Resource of Global Climate Data. *Nat. Clim. Data Center Tech. Rep.* **2001**. Available online: https://doi.org/http://Www1.Ncdc.Noaa.Gov/Pub/Data/Techrpts/Tr2000101/Tr2001-01.Pdf (accessed on 5 August 2020).
26. Galle, S.; Grippa, M.; Peugeot, C.; Moussa, I.B.; Cappelaere, B.; Demarty, J.; Mougin, E.; Panthou, G.; Adjomayi, P.; Agbossou, E.K.; et al. AMMA-CATCH, a Critical Zone Observatory in West Africa Monitoring a Region in Transition. *Vadose Zo. J.* **2018**, *17*, 1–24. [CrossRef]
27. Pfeifroth, U.; Kothe, S.; Müller, R.; Trentmann, J.; Hollmann, R.; Fuchs, P.; Werscheck, M. *Surface Radiation Data Set—Heliosat (SARAH)—Edition 2, Satellite Application Facility on Climate Monitoring*; EUMETSAT Satellite Application Facility on Climate Monitoring (CM SAF): Offenbach, Germany, 2017. [CrossRef]
28. Gbobaniyi, E.; Sarr, A.; Sylla, M.B.; Diallo, I.; Lennard, C.; Dosio, A.; Dhiédiou, A.; Kamga, A.; Klutse, N.A.B.; Hewitson, B.; et al. Climatology, Annual Cycle and Interannual Variability of Precipitation and Temperature in CORDEX Simulations over West Africa. *Int. J. Climatol.* **2014**, *34*, 2241–2257. [CrossRef]
29. Klein, C.; Heinzeller, D.; Bliefernicht, J.; Kunstmann, H. Variability of West African Monsoon Patterns Generated by a WRF Multi-Physics Ensemble. *Clim. Dyn.* **2015**, *45*, 2733–2755. [CrossRef]
30. Parker, D.J.; Diop-Kane, M. *Meteorology of Tropical West. Africa: The Forecasters' Handbook*, 1st ed.; John Wiley & Sons Ltd.: Chichester, UK, 2017. [CrossRef]
31. Brown, C.E. Coefficient of Variation. In *Applied Multivariate Statistics in Geohydrology and Related Sciences*; Springer: Berlin/Heidelberg, Germany, 1998; pp. 155–157. [CrossRef]

32. Ramanathan, V.; Cess, R.D.; Harrison, E.F.; Minnis, P.; Barkstrom, B.R.; Ahmad, E.; Hartmann, D. Cloud-Radiative Forcing and Climate: Results from the Earth Radiation Budget Experiment. *Science* **1989**, *243*, 57–63. [CrossRef]
33. Luiz, E.W.; Martins, F.R.; Gonçalves, A.R.; Pereira, E.B. Analysis of Intra-Day Solar Irradiance Variability in Different Brazilian Climate Zones. *Sol. Energy* **2018**, *167*, 210–219. [CrossRef]
34. Shivashankar, S.; Mekhilef, S.; Mokhlis, H.; Karimi, M. Mitigating Methods of Power Fluctuation of Photovoltaic (PV) Sources—A Review. *Renew. Sustain. Energy Rev.* **2016**, *59*, 1170–1184. [CrossRef]
35. Sultan, B.; Janicot, S. The West African Monsoon Dynamics. Part II: The "Preonset" and "Onset" of the Summer Monsoon. *J. Clim.* **2003**, *16*, 3407–3427. [CrossRef]
36. Nicholson, S.E. The ITCZ and the Seasonal Cycle over Equatorial Africa. *Bull. Am. Meteorol. Soc.* **2018**, *99*, 337–348. [CrossRef]
37. Nicholson, S.E. A Revised Picture of the Structure of the "Monsoon" and Land ITCZ over West Africa. *Clim. Dyn.* **2009**, *32*, 1155–1171. [CrossRef]
38. Sultan, B.; Janicot, S. Abrupt Shift of the ITCZ over West Africa and Intra-Seasonal Variability. *Geophys. Res. Lett.* **2000**, *27*, 3353–3356. [CrossRef]
39. Hayward, D.F.; Oguntoyinbo, J.S. *Climatology of West. Africa*; Hutchinson: London, UK, 1987.
40. Stein, T.H.M.; Parker, D.J.; Delanoë, J.; Dixon, N.S.; Hogan, R.J.; Knippertz, P.; Maidment, R.I.; Marsham, J.H. The Vertical Cloud Structure of the West African Monsoon: A 4 Year Climatology Using CloudSat and CALIPSO. *J. Geophys. Res. Atmos.* **2011**, *116*, 1–13. [CrossRef]
41. Bourgeois, E.; Bouniol, D.; Couvreux, F.; Guichard, F.; Marsham, J.H.; Garcia-Carreras, L.; Birch, C.E.; Parker, D.J. Characteristics of Mid-Level Clouds over West Africa. *Q. J. R. Meteorol. Soc.* **2018**, *144*, 426–442. [CrossRef]
42. Danso, D.K.; Anquetin, S.; Diedhiou, A.; Kouadio, K.; Kobéa, A.T. Daytime Low-Level Clouds in West Africa—Occurrence, Associated Drivers and Shortwave Radiation Attenuation. *Earth Syst. Dynam. Discuss.* **2020**. in review. [CrossRef]
43. Crouvi, O.; Schepanski, K.; Amit, R.; Gillespie, A.R.; Enzel, Y. Multiple Dust Sources in the Sahara Desert: The Importance of Sand Dunes. *Geophys. Res. Lett.* **2012**, *39*, 1–8. [CrossRef]
44. Knippertz, P.; Todd, M.C. Mineral Dust Aerosols over the Sahara: Processes of Emission and Transport, and Implications for Modeling. *Rev. Geophys.* **2012**, *50*, 28. [CrossRef]
45. Pfeifroth, U.; Sanchez-Lorenzo, A.; Manara, V.; Trentmann, J.; Hollmann, R. Trends and Variability of Surface Solar Radiation in Europe Based On Surface- and Satellite-Based Data Records. *J. Geophys. Res. Atmos.* **2018**, *123*, 1735–1754. [CrossRef]